

# **Aalborg Universitet**

# Opsonophagocytosis of Chlamydia pneumoniae by human monocytes and neutrophils

Lausen, Mads; Pedersen, Mathilde Selmar; Rahman, Nareen Sherzad Kader; Holm-Nielsen, Liv Therese; Farah, Faduma Yahya Mohamed; Christiansen, Gunna; Birkelund, Svend

Published in: Infection and Immunity

DOI (link to publication from Publisher): 10.1128/IAI.00087-20

Publication date: 2020

Document Version Accepted author manuscript, peer reviewed version

Link to publication from Aalborg University

Citation for published version (APA): Lausen, M., Pedersen, M. S., Rahman, N. S. K., Holm-Nielsen, L. T., Farah, F. Y. M., Christiansen, G., & Birkelund, S. (2020). Opsonophagocytosis of Chlamydia pneumoniae by human monocytes and neutrophils. *Infection and Immunity*, 88(7), Article e00087-20. https://doi.org/10.1128/IAI.00087-20

Copyright and moral rights for the publications made accessible in the public portal are retained by the authors and/or other copyright owners and it is a condition of accessing publications that users recognise and abide by the legal requirements associated with these rights.

- Users may download and print one copy of any publication from the public portal for the purpose of private study or research.
- You may not further distribute the material or use it for any profit-making activity or commercial gain
  You may freely distribute the URL identifying the publication in the public portal -

# Take down policy

If you believe that this document breaches copyright please contact us at vbn@aub.aau.dk providing details, and we will remove access to the work immediately and investigate your claim.

Downloaded from vbn.aau.dk on: December 05, 2025

IAI Accepted Manuscript Posted Online 13 April 2020

Copyright © 2020 American Society for Microbiology. All Rights Reserved.

Infect. Immun. doi:10.1128/IAI.00087-20

1

2

3	
4 5	Mads Lausen <sup>a</sup> , Mathilde Selmar Pedersen <sup>a</sup> , Nareen Sherzad Kader Rahman <sup>a</sup> , Liv Therese Holm-Nielsen <sup>a</sup> , Faduma Yahya Mohamed Farah <sup>a</sup> , Gunna Christiansen <sup>a,b</sup> , Svend Birkelund <sup>a#</sup>
6	
7 8	<sup>a</sup> Department of Health Science and Technology, Aalborg University, Fredrik Bajers Vej 3b, 9220 Aalborg Ø, Denmark
9	<sup>b</sup> Department of Biomedicine, Aarhus University, Wilhelms Meyers Allé 4, 8000 Aarhus, Denmark
10	*Corresponding author: sbirkelund@hst.aau.dk
11	
12	
13	
14	
15	
16	
17	
18	
19	
20	
21	
22	Word count abstract: 249
23	Word count main text: 4686
24	Running title: Opsonization and phagocytosis of C. pneumoniae
25	Keywords: Chlamydia pneumoniae, opsonization, phagocytosis, monocytes, neutrophils
26	

#### ABSTRACT

28

The human respiratory tract pathogen Chlamydia pneumoniae (C. pneumoniae) causing mild to severe 29 infections have been associated with the development of chronic inflammatory diseases. To understand 30 the biology of C. pneumoniae infections several studies have investigated the interaction between C. 31 32 pneumoniae and professional phagocytes. However, these studies have been conducted under nonopsonizing conditions making the role of opsonization in C. pneumoniae infections elusive. Thus, we 33 analyzed complement and antibody opsonization of C. pneumoniae and evaluated how opsonization 34 affects chlamydial infectivity and phagocytosis in human monocytes and neutrophils. 35 We demonstrated that IgG antibodies and activation products of complement C3 and C4 are deposited 36 on the surface of C. pneumoniae elementary bodies when incubated in human serum. Complement 37 38 activation limits C. pneumoniae infectivity in vitro and have the potential to induce bacterial lysis by formation of the membrane attack complex. Co-culture of C. pneumoniae and freshly isolated human 39 leukocytes showed that complement opsonization is superior to IgG opsonization for efficient 40 opsonophagocytosis of C. pneumoniae in monocytes and neutrophils. Neutrophil-mediated 41 phagocytosis of C. pneumoniae was crucially dependent on opsonization while monocytes retain minor 42 phagocytic potential under non-opsonizing conditions. Complement opsonization significantly 43 enhanced the intracellular neutralization of C. pneumoniae in peripheral blood mononuclear cells and 44 neutrophils and almost abrogated the infectious potential of C. pneumoniae. ' 45 46 In conclusion, we demonstrated that complement limits C. pneumoniae infection in vitro by interfering with C. pneumoniae entry into permissive cells, by direct complement-induced lysis and by tagging 47 bacteria for efficient phagocytosis in both monocytes and neutrophils. 48

Downloaded from http://iai.asm.org/ on April 15, 2020 at Aalborg University Library

#### INTRODUCTION

50

Chlamydia pneumoniae (C. pneumoniae) is a human pathogen frequently causing mild respiratory 51 symptoms during infection that usually resolves spontaneously but can cause severe, long-lasting 52 atypical pneumonia and has been associated with the development of several chronic disease conditions 53 54 including atherosclerosis and asthma (1, 2). C. pneumoniae is an obligate intracellular Gram-negative bacterium with a unique biphasic developmental cycle. The bacterium alternates between the 55 extracellular infectious elementary body (EB) and the intracellular non-infectious reticular body (RB). 56 During infection, C. pneumoniae EBs engage airway epithelium and induce their own uptake by 57 58 secreting pre-formed effectors into the host cell cytoplasm by the type-III secretion system (3). 59 Intracellularly, the EBs transform into RBs and start replicating in a modified vacuole called an inclusion. After 48-72 hours RBs start to divide asynchronously and EBs are formed and released from 60 the host cell by cell lysis or by membrane extrusion (4). 61 Upon infection, C. pneumoniae EBs first encounter airway epithelial cells and alveolar macrophages 62 63 which respond to infection by secreting inflammatory mediators stimulating vascular endothelium activation and immune cell chemotaxis (5). Neutrophil granulocytes are the first immune cells to 64 65 transmigrate from the blood stream into the alveolar space and subsequently signal for mononuclear cell recruitment and infiltration (6, 7). Thus, neutrophils and monocytes comprise an early cellular 66 defense against C. pneumoniae and the interaction between extracellular chlamydial EBs and these 67 68 phagocytes likely determines the course of the infection. Multiple studies have proposed that C. pneumoniae can evade intracellular killing mechanisms in both monocytes and neutrophils and thereby 69 70 use these cells as cellular vectors for extrapulmonary dissemination potentially causing chronic disease (8–10). However, these pro-survival mechanisms may be altered by the route of bacterial ingestion 71

93

trafficking pathways. 73 It was previously shown that phagocytic uptake of the intracellular bacterium Mycobacterium 74 tuberculosis (M. tuberculosis) through complement receptors or the mannose receptor protects the 75 76 bacterium from intracellular killing by delaying phagosome maturation (11, 12). On the contrary, 77 uptake of antibody opsonized M. tuberculosis trough Fcy-receptors causes rapid phagosome maturation and phagolysosomal fusion leading to reduced infection outcome. Thus, opsonin-directed phagocytosis 78 is a critical factor determining the intracellular fate of M. tuberculosis and similar mechanisms could be 79 80 involved in C. pneumoniae infections and pathogenesis, despite these pathogens being very different in 81 nature. 82 The complement system consists of more than 30 soluble and membrane-bound proteins that works in 83 a cascade-like manner to induce anti-microbial effector functions including opsonization, chemotaxis and cell lysis. The cascade process is initiated within minutes of engagement (13) and proceeds through 84 85 three separate activation pathways: Classical- (recognition of antibody complexes), lectin- (recognition of carbohydrate moieties), and alternative pathway (spontaneous hydrolysis of C3) (14). Following 86 activation, complement C4 and C3 are proteolytically cleaved into small soluble C4a/C3a fragments (9 87 kDa each) and large C4b/C3b fragments (75 kDa and 110 kDa, respectively) that attach covalently to 88 the activating surface and opsonize the microbe for phagocyte detection. C3b can be further cleaved 89 90 into iC3b, C3dg or C3d, which are all potent opsonins recognized by different complement receptors on phagocytic cells (14). The final stage of the complement cascade includes cleavage of complement 91 C5 and generation of a multimeric membrane-spanning C5b-9 complex (membrane attack complex, 92

Downloaded from http://iai.asm.org/ on April 15, 2020 at Aalborg University Library

since engagement with different phagocytic receptors activates different intracellular signaling and

MAC) that induces pore formation and cell lysis (14).

113

95	Although alveolar complement concentration and activity is reduced compared to concentrations and
96	activity seen in serum, the system is sufficiently functional to opsonize M. tuberculosis with
97	complement C3 activation products (15, 16). Primary infection leads to C. pneumoniae-specific IgG
98	production, but these antibodies offers limited protection against C. pneumoniae since reinfections are
99	frequently observed (17). Thus, during secondary infections both antibodies and complement are
100	present in the alveolar space, which have the potential to modulate the intracellular fate of $C$ .
101	pneumoniae in phagocytes and hence the outcome of the infection.
102	To further characterize the pathogenesis of <i>C. pneumoniae</i> during primary and secondary infections we
103	investigated how complement- and antibody opsonization affect phagocytosis and intracellular survival
104	of <i>C. pneumoniae</i> in human monocytes and neutrophils.
105	
106	
107	
108	
109	
110	
111	
112	

During primary infection, C. pneumoniae engages the complement system in the alveolar space.

Downloaded from http://iai.asm.org/ on April 15, 2020 at Aalborg University Library

# Infection and Immunity

# RESULTS

# Complement- and antibody opsonization of C. pneumoniae

To examine the role of opsonization and phagocytosis during <i>C. pneumoniae</i> infections, we first
screened the serum from 10 healthy donors for IgG antibodies against C. pneumoniae and found that
nine out of ten donors were positive for IgG against C. pneumoniae. Serum from one seropositive
individual and serum from the only identified seronegative individual were used in all further
experiments. These sera are called immune serum and non-immune serum, respectively, throughout
this paper.
Different cleavage fragments of complement C3 and C4 are known to bind and opsonize bacteria for
phagocytic recognition. C3 deposition on C. pneumoniae has only been investigated by flow cytometry
using an antibody recognizing various C3 cleavage forms (18). Thus, the exact C3 opsonins that bind
the C. pneumoniae surface remain unknown. In addition, complement C4 deposition has never been
investigated on C. pneumoniae. We therefore analyzed the deposition of these complement components
on purified C. pneumoniae EBs using immunoelectron microscopy (IEM) and western blotting.
Figure 1A demonstrates that complement C3 is abundantly deposited on the chlamydial surface when
incubated in non-immune serum (NHS-). Very limited C3 deposition was observed in heat-inactivated
serum (HIHS-) (Fig. 1B) suggesting that C3 deposition was due to activation of the complement system
and not due to unspecific antibody binding This observation was confirmed by quantification of gold
particles showing a median gold-binding ratio of 21.8 in NHS- (12.1-20.9) vs. 1.9 in HIHS- (1.2-2.6)
(Fig. 1C).

135

136

137

138

139

140

141

142

143

144

145

146

147

148

149

150

151

152

153

154

These observations were confirmed by western blot analysis demonstrating solid deposition of C3 in NHS-, but not in HIHS- (Fig. 1D). Several high molecular bands (above 110 kDa) are seen on the western blot, indicating cleavage of the alpha chain of native C3 and covalent attachment of C3 fragments to chlamydial surface structures (Fig. 1D). The 40 kDa fragment shown in Fig. 1D corresponds to the a'2 chain of C3, demonstrating deposition of the potent opsonin iC3b. Interestingly, we also demonstrated deposition of C4 on the chlamydial surface when incubated in NHS- (Fig. 1E), but not in HIHS- (Fig. 1F). Compared to C3, C4 was more sporadically deposited on the chlamydial surface indicated by a lower bacteria-to-background ratio for C4 (Fig. 1E+G). The observations were confirmed by western blot analysis which demonstrated deposition of the C4b opsonin. C4b deposition is indicated by the emergence of high molecular bands suggesting cleavage and exposure of the thioester group in the alpha chain of C4 along with the presence of the C4 beta- (70 kDa) and gamma chains (35 kDa) (Fig. 1H). These observations suggest involvement of the lectinmediated pathway since the non-immune serum tested negative for both anti-C. pneumoniae IgG and IgM making classical-mediated C4 activation unlikely. To evaluate opsonization during secondary infection we incubated C. pneumoniae EBs in immuneserum and investigated both antibody- and complement opsonization. Immunofluorescence microscopy demonstrated that immune serum reacted with individual chlamydial organisms located in perinuclear inclusions in infected HeLa cells (Fig. 2A). The IgG antibodies reacted with the surface of RBs indicated by the ring-shaped structures surrounding a DNA core (Fig. 2A). As expected, non-immune serum did not react with the chlamydial inclusions (Fig. 2B). These observations were made on fixed and permeabilized cells and may not accurately reflect native surface labeling.

156

157

158

159

160

161

162

163

164

165

166

167

168

169

170

171

172

173

174

175

176

Thus, to investigate native antibody labeling and to determine if antibodies in immune-serum also bind C. pneumoniae EBs, we incubated purified C. pneumoniae EBs with immune-serum and evaluated IgG binding to the surface by IEM. Gold-conjugated anti-human IgG antibodies bind to the surface of chlamydial EBs when incubated in immune-serum (Fig. 2C), while only few gold particles were associated with chlamydial EBs when incubated in non-immune serum (Fig. 2D). Quantitative analysis demonstrated a median gold-binding ratio of 27.1 (23.6-39.1) in HIHS+ vs. 1.1 (0.6-2.5) in HIHS-, showing that the limited bacterial gold deposition observed in non-immune serum equals the background gold deposition (Fig. 2E). Thus, human C. pneumoniae IgG antibodies present in serum interact with epitopes located both on fixed RBs (Fig. 2A) and native EBs (Fig. 2C+E). Next, we wanted to investigate if anti-C. pneumoniae IgG affects complement activation and deposition on the chlamydial surface. Complement C3 was heavily deposited when C. pneumoniae were incubated in NHS+, but not in HIHS+ (Fig. 2F-H). Similar levels of C3 deposition between immune serum and non-immune serum were observed (median ratios: NHS-: 21.8 vs. NHS+: 23.8) suggesting a negligible role of IgG in complement C3 deposition (Fig. 1A+C and Fig 2F+H). As expected, complement C4 was deposited on C. pneumoniae incubated in NHS+, but not in HIHS+ (Fig. 2J-L). More complement C4 deposition was observed in immune serum, in the presence of IgG, compared to non-immune serum (median ratios: NHS-: 3.5 vs. NHS+: 27.5) suggesting increased classical complement activation. Increased complement C4 deposition in immune serum compared to non-immune serum was also indicated by western blot analysis demonstrating more intense C4 bands when bacteria were incubated in immune-serum (Fig. 2M vs. Fig. 1H). Several high molecular bands were observed suggesting cleavage of the alpha chain of C4 and covalent attachment of C4b to the bacterial surface. In addition,

194

195

196

197

178	C4b (Fig. 2M).
179	In summary, C. pneumoniae is opsonized by iC3b and C4b in the absence of anti-C. pneumoniae IgG.
180	C. pneumoniae IgG is able to bind both EBs and RBs leading to increased C4b deposition on purified
181	EBs.
182	
183	Complement-mediated bacterial lysis
184	We wanted to investigate if the initial binding of complement and antibodies alone could interfere with
185	reproductive infection of C. pneumoniae, since antibody binding and complement activation precede
186	immune cell infiltration.
187	Electron microscopy revealed that most chlamydial organisms were intact after 30 minutes of
188	incubation in serum, demonstrating no signs of bacterial lysis (Fig. 3A). However, few bacteria showed
189	signs of complement-mediated lysis indicated by disruption of normal bacterial morphology together
190	with pore-forming structures (Fig. 3B, arrowheads). Thus, we aimed to investigate if the complement
191	cascade proceeds through the terminal complement pathway leading to MAC-induced bacterial lysis in
192	these cases. Chlamydial organisms were incubated in non-immune- and immune serum and
193	immunogold-labeled using a monoclonal antibody, recognizing a neoepitope of the C5b-9 complex. As

the cleaved alpha chain (a' chain) was observed around 80 kDa suggesting non-covalent attachment of

shown in Fig. 3C, C5b-9 is asymmetrically deposited on disintegrated chlamydial organisms and is

located in close proximity to 10 nm pore-like structures indicating MAC formation and MAC-induced

lysis. Bacteria incubated in heat-inactivated serum showed no signs of bacterial lysis (Fig. 3D). MAC

formation was observed in both immune- and non-immune serum, but more gold was observed in

199

200

201

202

203

204

205

206

207

208

209

210

211

212

213

214

215

216

217

218

219

NHS+ samples (median ratio: 34.5 (12.0-72.4)) compared to NHS- samples (median ratio: 12.1 (6.0-36.2)), suggesting that serum IgG promotes formation of C5b-9 complexes. Interestingly, most goldlabeled bacteria appeared healthy, with normal morphological features, and with no signs of bacterial lysis. These observations suggest that non-lytic C5b-9 complexes are formed on the chlamydial surface. Chlamydial organisms with altered morphology and signs of bacterial lysis appeared generally larger than unaffected chlamydiae possibly representing intermediate- or reticular bodies inevitably located within the EB fraction during the EB purification process. These observations imply that lytic C5b-9 formation occurs primarily on intermediate- or reticular bodies but leaving EBs unaffected. Thus, some C. pneumoniae organisms are sensitive to complement-mediated lysis in both immune and non-immune serum. Our observations show that complement fragments and antibodies deposit on almost all C. pneumoniae EBs while only few bacteria are directly killed by complement-mediated lysis. We therefore asked if opsonin deposition on apparently intact Chlamydia EB had any effect on chlamydial infectivity. To answer this question, we tested the ability of immune- and non-immune serum to neutralize chlamydial infection in HeLa cells by enumerating inclusion forming units (IFU) in each experimental condition. Figure 4 shows that complement had a significant impact on chlamydial infectivity. Only  $0.38\% \pm 0.2$ (mean  $\pm$  SD) and 1.19%  $\pm$  0.72 of the initial inoculum was recovered after incubation in immune-(NHS+) and non-immune serum (NHS-), respectively. These observations indicate that the combination of complement and antibodies more efficiently reduces chlamydial infectivity than complement alone, but the difference was not statistically significant. When serum was heat-inactivated  $19.1\% \pm 6.7$  and  $44.7\% \pm 5.8$  (Fig. 4) of inoculum was recovered demonstrating that complement significantly inhibits C. pneumoniae infectivity. The difference between heat-inactivated immune-

Downloaded from http://iai.asm.org/ on April 15, 2020 at Aalborg University Library

(HIHS+) and non-immune serum (HIHS-) further suggests that antibodies alone can reduce C. pneumoniae infectivity. To confirm this observation, we supplemented heat-inactivated non-immune serum (HIHS-) with the IgG fraction from a seropositive donor and evaluated chlamydial infectivity. As shown in Figure 4, supplementing non-immune serum with anti-C. pneumoniae IgG (HIHS-+IgG) significantly reduced chlamydial infectivity compared to non-immune serum alone confirming that anti-C. pneumoniae IgG reduces infectivity of C. pneumoniae. These data demonstrate that both antibody-, but especially complement opsonization have profound impact on C. pneumoniae infectivity.

228

229

230

231

232

233

234

235

236

237

238

239

240

220

221

222

223

224

225

226

227

# Complement-mediated phagocytosis of C. pneumoniae

As demonstrated above, neither complement- nor antibody opsonization completely abrogates chlamydial infectivity. We therefore aimed to investigate how phagocytes participate in the clearance of opsonized C. pneumoniae. To quantitatively evaluate the role of opsonization in phagocytic uptake during primary and secondary infections, we analyzed the uptake of opsonized and non-opsonized C. pneumoniae EB in monocytes and neutrophils by flow cytometry. Intracellular staining of cells for flow cytometry is troublesome as it requires cell permeabilization which causes considerable changes to physical characteristics of the cells. To avoid permeabilization C. pneumoniae organisms were labeled by FITC and uptake of FITC-labeled bacteria and FITC-labeling specificity were evaluated by confocal microscopy. Figure S1 shows that FITC-labeled organisms appear small (around 0.5 μm) and round in accordance with the morphology of chlamydial EBs. To confirm the intracellular location of these FITC-signals,

242

243

244

245

246

247

248

249

250

251

252

253

254

255

256

257

258

259

260

261

262

monocytes were stained for the cytoplasmic protein S100A8 to visualize the cell cytoplasm (Fig. S1B). As demonstrated in Fig. S1C all FITC-positive organisms are located inside the cell cytoplasm. FITC-labeling is a rather unspecific fluorescent labeling technique since the isothiocyanate group reacts with primary amine groups. Thus, to evaluate whether the FITC-signal in Fig. S1 originates from chlamydial organisms and not contaminants like cell debris from the chlamydial isolation procedure, we stained FITC-labeled chlamydiae with a monoclonal antibody against chlamydial LPS. As demonstrated in Fig. S1D+F all FITC-positive structures reacted with the anti-Chlamydia LPS antibody confirming that all FITC-positive structures are chlamydial organisms. Thus, FITC-labeling of C. pneumoniae is efficient and specific and the FITC-labeled bacteria locate inside the cells enabling the bacteria to be used in a flow cytometric assay. To analyze the effect of opsonization on phagocytosis of C. pneumoniae, isolated leukocytes were incubated with FITC-labeled C. pneumoniae in 30 min under different opsonizing conditions and subjected to flow cytometry analysis. To quantify the uptake, monocyte and neutrophil cell populations were gated as demonstrated in Fig. S2. Both cell types were gated based on forward- and side-scatter characteristics and monocytes were additionally gated based on CD14 surface expression. We first analyzed the role of complement-mediated opsonophagocytosis to experimentally mimic the infection conditions during primary infection. Thus, phagocytic uptake was quantified in medium containing either normal non-immune serum (NHS-) or heat-inactivated non-immune serum (HIHS-). As depicted in Fig. 5A+B, phagocytosis of C. pneumoniae in both monocytes and neutrophils is much more efficient in NHS- compared to HIHS- suggesting an important role for complement opsonization in phagocytosis of C. pneumoniae. Interestingly, neutrophil-mediated phagocytosis was almost absent under non-opsonizing conditions (Fig 5B, HIHS-), suggesting that opsononization is paramount for

neutrophil phagocytosis of C. pneumoniae while monocytes exploit opsonin-independent phagocytic pathways.

265

266

267

268

269

270

271

272

273

274

275

276

277

278

279

280

281

282

283

263

264

# Phagocytosis in the presence of anti-chlamydial antibodies

We demonstrated that monocyte- and especially neutrophil-mediated phagocytosis of C. pneumoniae were critically dependent on complement opsonization. Complement activation and activity in the alveolar space is reduced compared to serum and is primarily dependent on classical complement activation (15, 16). Thus, we sought to investigate whether anti-C. pneumoniae antibodies could mediate efficient phagocytosis or potentiate complement-mediated phagocytosis as both mechanisms may be important to understand the biology of C. pneumoniae reinfections. By comparing the heat-inactivated immune serum (Fig 5C+D, HIHS+) with heat-inactivated nonimmune serum (Fig 5A+B, HIHS-) it is evident that antibody opsonization increased phagocytic uptake of C. pneumoniae in both monocytes (3-fold increase) and especially in neutrophils (17-fold increase), however this effect was significantly lower compared to complement alone. To confirm these observations, we purified the IgG-fraction from immune serum and supplemented HIHS- with purified IgG. As demonstrated in Fig. 5E+F, supplementing non-immune serum with the IgG-fraction from immune serum increased the phagocytic uptake in both monocytes and neutrophils, confirming that the observed differences are due to anti-C. pneumoniae antibodies. We could not assess whether the presence of IgG potentiated complement-mediated phagocytosis since both monocyte and neutrophil cell populations were saturated with bacteria when complement competent serum was used (Fig. 5A-D, Downloaded from http://iai.asm.org/ on April 15, 2020 at Aalborg University Library

NHS+/-). We therefore re-analyzed these samples using C. pneumoniae at MOI=1 and showed that

monocytes and neutrophils more efficiently ingest C. pneumoniae when both complement and IgG antibodies are present (Fig. 5G+H).

286

287

288

289

290

291

292

293

294

295

296

297

298

299

300

301

302

303

304

284

285

# Intracellular survival of ingested bacteria

C. pneumoniae is ingested through both complement- and antibody dependent mechanisms. Evidence from other intracellular bacteria shows that the intracellular fate of ingested bacteria is highly dependent on the route of uptake, and it is therefore important to study the intracellular fate of C. pneumoniae under the opsonizing conditions we have demonstrated here. To evaluate the intracellular fate of ingested bacteria, PBMCs and neutrophils containing opsonized and non-opsonized bacteria were lysed by ultrasonication and liberated bacteria were used to infect HeLa cell monolayers. Statistically significantly less IFU were recovered when bacteria were ingested by PBMCs in the presence of immune serum (NHS+:  $45 \pm 19 \text{ IFU/}\mu\text{l}$ ) and non-immune serum (NHS-:  $70 \pm 16 \text{ IFU/}\mu\text{l}$ ) compared to bacteria ingested in media supplemented with heat-inactivated immune serum (HIHS+: 315 ±49 IFU/μl) and non-immune serum (HIHS-: 452 ±25 IFU/μl) (Fig. 6A). Similar results were obtained for neutrophils with 99  $\pm 4$  IFU/µl and 141  $\pm$  32 IFU/µl recovered IFU in immune- and nonimmune serum, respectively (Fig. 6B). Serum heat-inactivation caused a statistically significant increase in IFU recovery from both immune serum (Fig. 6B, HIHS+: 452 ±139 IFU/µl) and nonimmune serum (Fig. 6B, HIHS-:  $1151 \pm 259 \text{ IFU/}\mu\text{l}$ ). Although more bacteria are present intracellularly in cells incubated in NHS compared to HIHS (Figure 5A-D) more reproductive bacterial organisms can be recovered from cells in HIHS. These data suggest that complement not only facilitate Downloaded from http://iai.asm.org/ on April 15, 2020 at Aalborg University Library

306

307

308

309

310

311

312

313

314

315

rapid and efficient uptake of *C. pneumoniae*, but also mediates effective intracellular neutralization. We also observed statistically significant less IFU recovered from bacteria ingested in the presence of heat-inactivated immune serum (HIHS+) compared to heat-inactivated non-immune (HIHS-) in both cell types (Fig. 6A+B) suggesting that antibodies also play a role in bactericidal activity against C. pneumoniae. Studies performed on M. tuberculosis suggest that bacterial uptake by complement receptors delays phagosomal maturation and phagolysomal fusion thereby facilitating intracellular bacterial survival. Our results suggest the opposite; that complement-mediated uptake leads to rapid intracellular neutralization of C. pneumoniae. We therefore tested whether C. pneumoniae were targeted to lysosomal compartments in monocytes after complement-mediated ingestion. Figure 6C-E shows that C. pneumoniae localizes within LAMP1-positive vesicular structures in monocytes after 30 min (Fig. 6F). Thus, complement-mediated uptake of C. pneumoniae in monocytes directs ingested bacteria

# Infection and Immunity

# DISCUSSION

In the present study, we demonstrated that C. pneumoniae EBs are opsonized with both IgG and the
complement opsonins iC3b and C4b when incubated in human serum. We showed that complement
activation limits C. pneumoniae infection in multiple ways by interfering with C. pneumoniae entry
into permissive cells, by direct MAC-induced lysis and by tagging bacteria for efficient phagocytosis
by both monocytes and neutrophils.
The activation and deposition of complement C3 and the terminal complement complex on <i>C</i> .
pneumoniae demonstrated in this study were previously shown by Cortes and colleagues (18).
Interestingly, using electron microscopy, we observed C5b-9 deposition without pore-formation and
bacterial lysis. C5b-9 complexes associated with pore-like structures and altered bacterial morphology
were primarily observed on reticular- and intermediate bodies. Thus, our observations suggest that
extracellular EBs may be resistant to MAC-induced lysis. It is likely, that the cysteine-rich proteins in
the highly cross-linked chlamydia outer membrane of EBs provide a physical barrier that hinders
components of the terminal complement complex to interact with the outer membrane lipid bilayer.
Alternatively, MAC formation could be inhibited by recruitment of host-derived complement
regulators to the EB surface. Thus, it was previously demonstrated that C. trachomatis binds the MAC
inhibitor vitronectin, however, it was not investigated if vitronectin modulates complement deposition
on the chlamydial surface (19).
Cortes et al. concluded that properdin and alternative complement activation was indispensable for C31
deposition and complement-mediated neutralization. Interestingly, we found that complement C4 is
deposited on the surface of C. pneumoniae. Deposition of complement C4 in both immune- and
nonimmune serum suggests that also the lectin-mediated activation pathway is involved in C

349

350

351

352

353

354

355

356

357

358

359

360

361

362

363

364

365

366

367

368

369

pneumoniae induced complement activation. This observation is supported by previous studies demonstrating that different lectins can bind the surface of C. pneumoniae (20, 21). Moreover, quantification of gold-labeling and semi-quantitative western blot analysis suggested that more C4 was deposited in immune serum compared to non-immune serum, indicating activation of the classical pathway. This is supported by the finding that IgG1 is the predominant IgG subclass raised against C. pneumoniae and to a lesser extend IgG3 and both IgG1 and IgG3 are efficient complement activators (22). The IgG subclasses raised against C. pneumoniae may also explain why we observe an IgGdependent inhibition of C. pneumoniae infectivity in HeLa cells (Fig. 4). Studies on C. trachomatis showed that HeLa cells express FcyRIII and that Fc-mediated endocytosis through this receptor promotes reproductive infection of C. trachomatis (23, 24). It is likely that C. trachomatis is more prone to FcyRIII-mediated uptake compared to C. pneumoniae since IgG3 is the predominant IgG subclass raised against C. trachomatis (22). Thus, the IgG subclass distribution seems important for the infectivity and reproductive outcome of *Chlamydia spp. in vitro*. A possible explanation for the discrepancies between our results and the findings by Cortes et al. could be that classical- and/or lectin-mediated activation pathways are abrogated at the C4 level leading to pathway termination before C3 cleavage. C4 binding protein (C4bp), a fluid-phase negative complement regulator, can terminate complement activation at the C4 level by inducing C4b cleavage and C2a dissociation from the classical C3 convertase (25). Several bacterial pathogens are able to recruit and bind C4bp leading to complement resistance, but this has not yet been demonstrated for chlamydial organisms (26, 27). The alternative activation pathway seems important for C. pneumoniae-induced complement activation in vitro but the significance of this pathway during in vivo lung infections is still elusive. In the lungs,

371

lavage fluid (15, 28). It remains uncertain whether C. pneumoniae is opsonized in the alveolar space of 372 the lungs, but the classical complement activation is functional, and during secondary infection 373 complement activating IgG is present in the alveolar space (15). 374 We show that complement efficiently facilitates phagocytosis of C. pneumoniae in both monocytes and 375 neutrophils and that most opsonized bacteria are unable to cause reproductive infection when liberated 376 from phagocytes. Complement receptor 3 (CR3, CD11b/CD18) recognizes different C3 cleavage 377 378 fragments including iC3b identified on C. pneumoniae EBs here. CR3 is, together with Fcy-receptors, 379 the most important phagocytic receptor and is widely expressed on both monocytes and neutrophils. It is, therefore, likely that complement-mediated phagocytosis takes place via CR3 leading to intracellular 380 destruction. This is different from CR-mediated uptake of other intracellular bacteria. CR-mediated 381 uptake of M. tuberculosis into human monocytes and macrophages allow safe entrance by delaying 382 phagosomal maturation and phagolysosomal fusion (11). We observed that C. pneumoniae is rapidly 383 384 targeted to LAMP1-positive intracellular compartments showing efficient phagosomal trafficking 385 facilitating intracellular neutralization of the chlamydial reproductive potential. Thus, safe entrance into host cells through CR-mediated phagocytosis is not a conserved mechanism for all intracellular 386 bacteria. This is supported by the observation that the facultative intracellular bacterium Francisella 387 tularensis (F. tularensis) fails to escape phagosomal trafficking in murine bone-marrow macrophages 388 389 when opsonized with either complement or IgG (29). Knockout of CD11b, a subunit of the heterodimeric CR3, leads to phagosomal escape with cytosolic localization of F. tularensis, supporting 390 391 that CR3 plays opposing roles during experimental infections with different intracellular bacteria (29).

complement activation proceeds primarily through the classical pathway and alternative complement

activation fails to activate and deposit C3 on both mycobacteria and streptococci in bronchoalveolar

393

394

395

396

397

398

399

400

401

402

403

404

405

406

407

408

409

410

411

412

413

Direct interaction between opsonized bacteria and phagocytic opsonin-receptors provides one explanation for the increased phagocytic uptake and intracellular neutralization observed here. Phagocytic priming by the complement anaphylatoxins C3a and C5a may provide another likely explanation. In an in vivo C. psittaci lung infection model C5aR--- mice displayed slightly worsened clinical score compared to WT during early stage infection (30). The same authors later demonstrated that C3a and its receptor C3aR are critically involved in anti-chlamydial immunity in the same C. psittaci lung infection model (31). Both receptors are expressed on monocytes and neutrophils and can potentiate phagocytic functions by inducing both an increased surface expression of complement receptors and induce a hostile intracellular environment (32, 33). C5a induces increased surface expression of CD11b and increased phagocytosis of Escherichia coli (E. coli) in neutrophils (34) and can also potentiate intracellular killing of E. coli by increasing the oxidative burst in a whole blood assay (35). In addition, priming neutrophils with C5a leads to translocation of CR1 containing secretory vesicles to the cell surface (36, 37). CR1 recognizes the activation products C3b and C4b together with several other complement-related proteins (38). We demonstrate for the first time, that C4b is deposited on the surface of C. pneumoniae and hence, C5a-induced translocation of CR1 to the plasma membrane may induce increased bacterial phagocytosis. However, the role of C4b in opsonophagocytosis remains elusive. We demonstrated that C. pneumoniae ingested in the presence of complement-competent serum had impaired ability to cause reproductive infection in HeLa cells compared to bacteria ingested under nonopsonizing conditions. Intracellular survival and replication of C. pneumoniae within phagocytes have previously been evaluated in several in vitro studies; however, these have been conducted under

415

416

417

418

419

420

421

422

423

424

425

426

427

428

429

430

431

432

433

434

various experimental conditions. Both C. pneumoniae and C. trachomatis are able to replicate in human neutrophils when ingested under non-opsonizing conditions (10, 39). Rajeeve et al. showed that C. trachomatis uses the chlamydial protease-like activating factor (CPAF) to inhibit neutrophil activation and cell death thereby creating a replicative environment (39). Since CPAF is highly conserved among chlamydiae, C. pnuemoniae may use a similar CPAF-dependent mechanism to survive and replicate in neutrophils. Similarly, co-incubating monocytes and C. pneumoniae under non-opsonizing conditions leads to recovery of chlamydial progeny up until 48 hours post infection (9, 40) suggesting that opsoninindependent uptake also facilitates C. pneumoniae survival in monocytes. This idea was further supported by the observation that differentiated macrophages support intracellular replication of C. pneumoniae. Differentiated macrophages, but not peripheral blood monocytes, express the mannose receptor (MR) which facilitate intracellular survival of M. tuberculosis, and MR has also been linked to phagocytic uptake of chlamydial organisms (12, 41, 42). Others used commercially available human serum from AB blood type donors in the infection medium combined with centrifugation. These studies were unable to recover chlamydial progeny after 6 and 48 hours, but detected 16S rRNA suggesting metabolic, but not replicative activity (8, 43). However, neither complement functional activity nor serostatus were evaluated for these sera making it difficult to draw any conclusions on the role of opsonization. We demonstrated that both complement- and IgG-opsonization potentiates phagocytosis and intracellular killing of C. pneumoniae suggesting that the uptake mechanism is important for the intracellular fate of C. pneumoniae previously demonstrated for other chlamydial organisms (44).

C. pneumoniae progeny infection and facilitates C. pneumoniae uptake in human monocytes and neutrophils. Ingested bacteria are rapidly trafficked to destructive intracellular compartments and eliminated showing that opsonization and phagocytosis are efficient means of controlling extracellular C. pneumoniae organisms. Thus, opsonization is a critical factor to include in future in vitro studies exploring the interaction between C. pneumoniae and human phagocytes.

Here we demonstrated that complement opsonization and to a lesser extend IgG opsonization inhibits

455

474

# MATERIALS AND METHODS

Antibodies	and	reagents
<i>i</i> minimounce	anu	I Cagciiu

456	The following primary antibodies were used in this study: PE anti-human CD14 (Clone: M5E2)
457	(BioLegend, CA, USA), MAb 15.2.3 against chlamydial LPS (45), PAb198 against C. pneumoniae
458	outer membrane (46), Anti-MRP8 (S100A8) (Abcam, UK), Anti-LAMP1 (Sino Biological, China),
459	Polyclonal Rabbit Anti-Human C3c (Agilent Technologies, Glostrup, Denmark), Polyclonal Rabbit
460	Anti-Human C4c (Agilent) and Monoclonal Mouse Anti-Human C5b-9 (clone aE11, Agilent).
461	The following secondary antibodies were used in this study: Goat anti human IgG-, Goat anti rabbit
462	and Goat anti mouse antibody conjugated to 10 nm colloidal gold (British BioCell, Cardiff, UK) was
463	used for immunoelectron microscopy. Horseradish peroxidase conjugated Affinipure Goat Anti-Human
464	Fcγ-specific IgG was used for ELISA. Anti-Rabbit IgG conjugated to alkaline phosphatase was used
465	for western blotting (Sigma Aldrich, MO, USA). FITC-conjugated Goat Anti-Human IgG, Fcγ
466	fragment specific (Jackson ImmunoResearch, Cambridge, UK), Alexa Fluor® (AF) 555 goat anti-
467	rabbit, AF555 goat anti-mouse and AF647 goat anti-rabbit (Invitrogen, Thermo Fisher Scientific, MA,
468	USA) were used for immunofluorescence staining.
469	TMB/ONE (3,3',5, 5'-tetramethylbenzidine) and BCIP/NBT (5-bromo-4-chloro-3-indolyl phosphate/
470	Nitro Blue Tetrazolium) were purchased from Kementec (Kementec, Taastrup, Denmark) and used for
471	ELISA and western blotting, respectively.
472	
473	

Cell	lines	and	cul	ture

BHK- and HeLa cell lines were purchased from the American Type Culture Collection (ATCC, VA, 476 USA) and cultured in complete medium consisting of RPMI 1640 supplemented with 5% fetal calf 477 serum (FCS), and 0.01 mg/ml gentamicin and maintained at 37°C and 5% CO<sub>2</sub>. Cell lines were tested 478 free of mycoplasma by Hoechst (33258) staining. 479

480

481

482

483

484

485

486

475

# Bacterial organism and propagation

C. pneumoniae (CDC/CWL-029/VR1310) was purchased from ATCC and cultivated in Baby Hamster kidney (BHK) cells in complete medium added 2 μg/ml cycloheximide and 0.1% glucose. The infected cells were cultured at 37°C and 5% CO2 for 72 hours. C. pneumoniae EBs were purified by density gradient centrifugation as previously described (46). Mock inoculum was prepared by processing uninfected BHK cells in parallel with infected cells.

487

488

489

490

491

492

493

494

#### Serum samples

Serum was obtained from 10 healthy volunteers at Aalborg University, Denmark. Blood was drawn by venipuncture and collected in S-Monovette® serum tubes (Sarstedt, Nümbrecht, Germany) and serum was isolated immediately according to manufactures instructions. Isolated serum was immediately stored on ice before freezing at -80 °C for later use. Serum heat inactivation was done for 30 min at 56°C. Serum containing anti-C. pneumoniae IgG is denoted "immune serum" and serum without anti-C. pneumoniae IgG is denoted "non-immune serum". Throughout this paper the following

496

497

498

499

500

501

502

503

504

505

506

507

508

509

510

511

512

513

514

515

abbreviations will be used described the different sera: NHS+: Immune serum, NHS-: Non-immune serum, HIHS+: heat-inactivated immune serum and HIHS-: heat-inactivated non-immune serum. All protocols were approved by the Regional ethics committee of Region Nordjylland (N-20150073) and all experiments were carried according to the Declaration of Helsinki. All participants gave written informed consent to participate in the study. **ELISA** C. pneumoniae specific IgG was measured using Chlamydia pneumoniae-IgG ELISA Medac plus (Medac, Wedel, Germany) using C. pneumoniae outer membrane complex as antigen. Absorbance were measured at 450 nm on a Sunrise TM microplate reader (Tecan, Mannedorf, Switzerland). Immunofluorescence validation of serum reactivity HeLa cell monolayers, seeded on coverslips, were infected with 5x10<sup>5</sup> inclusion forming units (IFU) C. pneumoniae by centrifugation at 1000 x g for 30 min at 37°C followed by 30 min incubation at 37°C and 5% CO<sub>2</sub>. Medium containing extracellular bacteria was removed and cells were incubated in complete medium added 2 µg/ml cycloheximide and 0.1% glucose for 48 hours and subsequently fixed in 3.7% formaldehyde for 20 min at 4 °C. Cells were permeabilized in ice cold methanol for 10 min, blocked in 0.5% bovine serum albumin (BSA) for 15 min at 37°C and incubated with serial dilutions of

Downloaded from http://iai.asm.org/ on April 15, 2020 at Aalborg University Library

immune- and non-immune serum for 30 min at 37°C. Cells were washed three times in PBS and

incubated with FITC-conjugated anti-human IgG secondary antibody diluted 1:200 in 0.1% BSA in

PBS for 30 min at 37°C. Cells were washed three times in PBS and counter stained with using 2  $\mu$ M

To-Pro-3 Iodide (Invitrogen, Thermo Fisher Scientific) for 20 min at room temperature. Cells were imaged using a Leica TCS SP5 confocal laser scanning microscope with a HCX PL Apo 63x/1.40 and CX PL Apo 100x/1.47 objective (Leica Microsystems, Wetzlar, Germany).

519

520

521

522

523

524

525

526

527

528

529

530

531

532

533

534

535

536

537

516

517

518

# Immunogold-labeling and transmission electron microscopy (TEM)

Purified C. pneumoniae EBs were incubated in 50% NHS or HIHS for 30 min at 37°C and washed three times in PBS with centrifugation at 15.000 x g, for 15 min at 4°C between each wash. Processing and immunogold-labeling of bacteria for TEM was performed as previously described (47). Briefly, serum coated (NHS or HIHS) C. pneumoniae EBs were added to carbon coated 400-mesh glowdischarged nickel grids and washed three times in PBS before blocking in 1% ovalbumin (Sigma-Aldrich) in PBS (pH 6.5). To determine binding of human antibodies to the chlamydial surface, grids were incubated for 30 min at 37°C with Goat anti human IgG conjugated to 10 nm colloidal gold diluted 1:25 in 0.5% ovalbumin in PBS. To determine complement binding, samples were incubated with primary antibodies (anti-C3c, 1:200; anti-C4c, 1:200; anti-C5b-9, 1:20) diluted in 0.5% ovalbumin in PBS for 30 min at 37°C. Grids were washed in three drops of PBS and subsequently incubated for 30 min at 37°C with secondary antibodies (Goat anti rabbit or Goat anti mouse antibody conjugated to 10 nm colloidal gold) diluted 1:25 in 0.5% ovalbumin in PBS. The grids were washed in three drops PBS, incubated in three drops of 0.5% cold fish gelatin in PBS and negatively stained with 0.5% phosphotungstic acid (PTA). Grids were blotted dry on filter paper and investigated using a Jeol 1010 transmission electron microscope (Jeol, Tokyo, Japan). Gold-deposition was quantified as previously described (47). Briefly, a minimum of seven random fields were imaged for each grid containing at least 12 chlamydial organisms in total. For each chlamydial organism, gold particles on the bacteria

Downloaded from http://iai.asm.org/ on April 15, 2020 at Aalborg University Library

Downloaded from http://iai.asm.org/ on April 15, 2020 at Aalborg University Library

and in the background were counted and the density of deposition was calculated for both (gold per area). From these numbers, a bacteria-to-background ratio was calculated to quantitatively describe bacterial gold deposition relative to background deposition. From these ratios the median and interquartile ranges (IQR) were calculated for each sample.

SDS-PAGE and western blotting were performed essentially according to Lausen et al. (47). Briefly,

542

543

544

545

546

547

548

549

550

551

552

553

554

555

556

538

539

540

541

# Western blotting

purified C. pneumoniae EBs were incubated in 50% serum for 30 minutes at 37°C and unbound complement was removed by washing three times in PBS with centrifugation at 15,000 x g for 15 min between each wash. The chlamydial pellet was lysed in SDS Sample buffer + 5% β-mercaptoethanol and proteins were separated on an 8 % polyacrylamide gel. Proteins were blotted on to a nitrocellulose membrane (GE Healthcare Life Sciences IL, USA) in Tris-Glycine buffer (25 mM Tris, 192mM glycine) + 20% methanol for two hours at 100 V using a TE22 Mighty Small Transfer Tank (Hoefer, Inc., Holliston, MA). Membranes were blocked for 30 min at 37°C in 3% gelatin in Tris-buffered saline (TBS). Antibodies diluted in TBS + 0.05% Tween-20 (TBST) + 0.2% gelatin were added to the membranes and left for incubation for one hour at 37°C. Blots were washed three times in TBST and incubated with alkaline phosphatase-conjugated secondary antibody for one hour at 37°C. Antigen-antibody complexes were visualized by adding BCIP/NBT (Kementec) alkaline phosphatase substrate.

557

558

# Serum neutralization assay

C. pneumoniae EBs were incubated in RPMI 1640 supplemented with 10% human serum for 30 min at 37°C. Opsonized bacteria (10.8x10<sup>4</sup> IFU for NHS samples and 1.2x10<sup>4</sup> IFU for HIHS samples) were used to infect HeLa cell monolayers as described above. Cells were processed for immunofluorescence microscopy as described above with minor modifications. PAb198 (1:400) and FITC-conjugated goat anti-rabbit (1:200) were used as primary and secondary antibodies, respectively, and cell nuclei were stained with 2 µg/ml DAPI. The cells were inspected using a Leica LSM550 fluorescence microscope and images were captured from seven random fields in each sample. All samples were analyzed in duplicates and repeated in three independent experiments. The number of IFU was enumerated and expressed as percentage of initial inoculum. Data from the three experiments are expressed as mean ± standard deviation (SD).

Downloaded from http://iai.asm.org/ on April 15, 2020 at Aalborg University Library

570

571

572

573

574

575

576

577

559

560

561

562

563

564

565

566

567

568

569

# FITC-labelling of bacteria

C. pneumoniae inoculum was suspended in 0.1 M NaHCO<sub>3</sub> (pH = 9) and centrifuged for 15 min at 15.000 x g. Fluorescein isothiocyanate isomer 1 (FITC) (Sigma, MO, USA) was added at a concentration of 0.1 mg/ml in 0.1 M NaHCO<sub>3</sub> buffer and bacteria were incubated for one hour protected from light. The labeled bacteria were washed three times in PBS to remove unbound FITC and the final bacteria pellet was suspended in sucrose-phosphate buffer (2SP), aliquoted, and stored at -80°C.

578

579

# Immune cell isolation and culture

Peripheral blood was obtained from two donors (one seropositve and one seronegative) and collected in S-Monovette (Sarstedt) EDTA tubes. Blood was layered on Polymorphprep<sup>TM</sup> density gradient medium (Axis-Shield, Dundee, UK) and centrifuged for 40 min at 300 x g at 20°C. Layers with peripheral blood mononuclear cells (PBMCs) and polymorphnuclear cells were harvested and collected in the same tube when used for flow cytometry. The two cell populations were kept separate when used for immunofluorescence microscopy. Platelets was removed by centrifugation at 120 x g for 10 min at 20°C. Cells were resuspended in complete RPMI 1640 medium.

588

589

590

591

592

593

594

595

596

597

598

599

580

581

582

583

584

585

586

587

# Immunofluorescence staining and microscopy of immune cells

For immunofluorescence staining, PBMCs were seeded in 8-well Nunc® Lab-Tek® Chamber<sup>TM</sup> slides with a density of 9 x 10<sup>5</sup> cells/well. Cells were left to adhere for 90 min and non-adherent cells were removed by washing twice in PBS. Bacteria were added at a multiplicity of infection (MOI) 10 in RPMI 1640 + 10% human serum. Non-phagocytized bacteria were removed by washing three times in PBS and cells were processed for immunofluorescence staining as described above. PAb198 (1:400), anti-LAMP1 (1:400), anti-S100A8 (1:300) and MAb 15.2.3 (1:20) were used as primary antibodies and AF555-conjugated goat antimouse, AF555-conjugated goat anti-rabbit and AF647-conjugated goat anti-rabbit were used as secondary antibodies in an 1:200 dilution. Cell nuclei were stained using 2 µM To-Pro-3 Iodide (Invitrogen, Thermo Fisher Scientific). Cells were imaged using a Leica TCS SP5 confocal laser

Downloaded from http://iai.asm.org/ on April 15, 2020 at Aalborg University Library

601

602

603

604

605

606

607

608

609

610

611

612

613

614

615

616

617

618

619

scanning microscope with a CX PL Apo 100x/1,47 objective (Leica Microsystems). Phagocytosis assay FITC-labeled C. pneumoniae EBs were opsonized in RPMI 1640 + 10% human serum for 15 min at 37°C. Bacteria (1x10<sup>7</sup> or 1x10<sup>6</sup> bacteria/tube) and immune cells (1x10<sup>6</sup> cells/tube) were mixed in 5 ml polypropylene tubes (MOI=10 and MOI=1, respectively) and co-incubated for 30 min at 37°C and cells were subsequently processed for flow cytometry. Flow cytometry Cells were washed in cold PBS + 0.05% sodium azide to remove non-phagocytized bacteria. Fcreceptors were blocked using 20 μg/ml human IgG (Sigma) for 15 min at 4°C. Primary fluorochromeconjugated antibodies, diluted in PBS + 0.05% sodium azide + 0.01% BSA, were added and cells were stained for 30 min at room temperature. Unbound antibody was removed by washing in PBS and cell viability was assessed using eBioscience TM Fixable Viability dye eFluor A50 according to manufacturers's instructions. The cells were washed twice in PBS and fixed in 1% formaldehyde for 20 min at 4°C and analyzed on a CytoFLEX flow cytometer (Beckman Coulter, CA, USA). **IgG** purification

Serum from one seropositive donor was mixed 1:1 with binding buffer (1 M glycine, 150 mM NaCl,

pH 8.5) and the serum IgG fraction was isolated on an affinity chromatography column packed with

621

622

623

624

625

626

627

628

629

630

631

632

633

634

635

636

637

638

639

USA).

GammaBind Plus protein G Sepharose (GE Healthcare). Bound IgG was eluted from the column using elution buffer containing 100 mM glycine-HCl pH 2.7 and collected in 25 fractions in tubes containing 1 M Tris-HCl pH 9 to restore neutral pH. The protein concentration in each fraction was determined using Pierce<sup>TM</sup> BCA Protein Assay Kit (Thermo Scientific) according to manufacturer's instruction. Intracellular survival assay PBMCs and neutrophils were co-incubated with bacteria as described above. Cells were washed three times in PBS to remove non-phagocytized bacteria. The cell pellet was suspended in 2SP buffer and cells were lysed by ultrasonication to liberate ingested bacteria. The cell lysates were used to infect HeLa cells and IFU were quantified from duplicate samples in three independent experiments as described above. **Data analysis** Flow cytometry data were analyzed using FlowLogic<sup>TM</sup> v.7.2.1 (Inivai Technologies, Mentone Victoria, Australia). One-way ANOVA with Tukey's post hoc or Welch ANOVA with Games-Howell multiple comparison test was used to investigate differences between multiple means. Differences between means from two independent groups were investigated using student's independent t-test or

Downloaded from http://iai.asm.org/ on April 15, 2020 at Aalborg University Library

Welch's t-test. All statistical analyses were performed in SPSS Statistics 25 (IBM, Armonk, NY,

ACKNOWLEDGEMENTS

661 662

641	We would like to thank Ditte Bech Laursen for technical assistance. This study was funded by Aase
642	and Ejner Danielsen foundation, the Obel Family Foundation and by the Joint Strategic Research
643	Programme on Fighting antibiotic Resistance (Aalborg University and University of Southern
644	Denmark)
645	
646	CONFLICT OF INTEREST
647	The authors declare no conflict of interest.
648	
649	
650	
651	
652	
653	
654	
655	
656	
657	
658	
659	
660	

REFERENCES

663

- Porritt RA, Crother TR. 2017. Chlamydia pneumoniae Infection and Inflammatory 1. 664
- Diseases. For Immunopathol Dis Therap 7:237–254. 665
- Grayston JT, Belland RJ, Byrne GI, Kuo CC, Schachter J, Stamm WE, Zhong G. 2. 666
- 2015. Infection with Chlamydia pneumoniae as a cause of coronary heart disease: the 667
- 668 hypothesis is still untested. Pathog Dis **73**:1–9.
- Elwell C, Mirrashidi K, Engel J. 2016. Chlamydia cell biology and pathogenesis. Nat 669 3.
- Rev Microbiol 14:385-400. 670
- 4. Zuck M, Sherrid A, Suchland R, Ellis T, Hybiske K. 2016. Conservation of extrusion 671
- as an exit mechanism for Chlamydia. Pathog Dis 74:ftw093. 672
- Jahn H, Krüll M, Wuppermann FN, Klucken AC, Rosseau S, Seybold J, Hegemann 5. 673
- JH, Jantos CA, Suttorp N. 2000. Infection and Activation of Airway Epithelial Cells by 674
- Chlamydia pneumoniae. J Infect Dis 182:1678–1687. 675
- Gieffers J, van Zandbergen G, Rupp J, Sayk F, Krüger S, Ehlers S, Solbach W, 6. 676
- 677 Maass M. 2004. Phagocytes transmit Chlamydia pneumoniae from the lungs to the
- vasculature. Eur Respir J 23:506–510. 678
- Chiba N, Shimada K, Chen S, Jones HD, Alsabeh R, Slepenkin A V, Peterson E, 7. 679
- Crother TR, Arditi M. 2015. Mast cells play an important role in chlamydia 680
- pneumoniae lung infection by facilitating immune cell recruitment into the airway. J 681

- 682 Immunol **194**:3840–51.
- 8. Buchacher T, Wiesinger-Mayr H, Vierlinger K, Rüger BM, Stanek G, Fischer MB, 683
- Weber V. 2014. Human blood monocytes support persistence, but not replication of the 684
- 685 intracellular pathogen C. pneumoniae. BMC Immunol 15:60.
- 9. Marangoni A, Bergamini C, Fato R, Cavallini C, Donati M, Nardini P, Foschi C, 686
- Cevenini R. 2014. Infection of human monocytes by Chlamydia pneumoniae and 687
- Chlamydia trachomatis: an in vitro comparative study. BMC Res Notes 7:230. 688
- van Zandbergen G, Gieffers J, Kothe H, Rupp J, Bollinger A, Aga E, Klinger M, 689 10.
- Brade H, Dalhoff K, Maass M, Solbach W, Laskay T. 2004. Chlamydia pneumoniae 690
- Multiply in Neutrophil Granulocytes and Delay Their Spontaneous Apoptosis. J 691
- Immunol 172:1768-1776. 692
- 693 11. Schlesinger LS. 1996. Entry of Mycobacterium tuberculosis into mononuclear
- phagocytes. Curr Top Microbiol Immunol 215:71–96. 694
- 12. Kang PB, Azad AK, Torrelles JB, Kaufman TM, Beharka A, Tibesar E, DesJardin 695
- LE, Schlesinger LS. 2005. The human macrophage mannose receptor directs 696
- Mycobacterium tuberculosis lipoarabinomannan-mediated phagosome biogenesis. J Exp 697
- Med 202:987-99. 698
- 13. Jensen TS, Opstrup K V., Christiansen G, Rasmussen P V., Thomsen ME, Justesen 699
- DL, Schønheyder HC, Lausen M, Birkelund S. 2020. Complement mediated 700

- 701 Klebsiella pneumoniae capsule changes. Microbes Infect 22:19–30.
- Merle NS, Church SE, Fremeaux-Bacchi V, Roumenina LT. 2015. Complement 702 14.
- 703 System Part I - Molecular Mechanisms of Activation and Regulation. Front Immunol
- 704 **6**:262.
- Ferguson JS, Weis JJ, Martin JL, Schlesinger LS. 2004. Complement protein C3 705 15.
- binding to Mycobacterium tuberculosis is initiated by the classical pathway in human 706
- bronchoalveolar lavage fluid. Infect Immun 72:2564–2573. 707
- Bolger MS, Ross DAS, Jiang H, Frank MM, Ghio AJ, Schwartz DA, Wright JR. 708 16.
- 2007. Complement levels and activity in the normal and LPS-injured lung. Am J Physiol 709
- Lung Cell Mol Physiol 292:748–759. 710
- 711 17. Gaede KI, Wilke G, Brade L, Brade H, Schlaak M, Müller-Quernheim J. 2002.
- 712 Anti-Chlamydophila immunoglobulin prevalence in sarcoidosis and usual interstitial
- pneumoniae. Eur Respir J 19:267–274. 713
- 18. Cortes C, Ferreira VP, Pangburn MK. 2011. Native properdin binds to Chlamydia 714
- pneumoniae and promotes complement activation. Infect Immun **79**:724–731. 715
- 19. Kihlström E, Majeed M, Rozalska B, Wadström T. 1992. Binding of Chlamydia 716
- trachomatis serovar L2 to collagen types I and IV, fibronectin, heparan sulphate, laminin 717
- and vitronectin. Zentralbl Bakteriol 277:329-33. 718
- 20. Swanson AF, Kuo CC. 1990. Identification of lectin-binding proteins in Chlamydia 719

- 720 species. Infect Immun 58:502-7.
- Swanson AF, Ezekowitz RA, Lee A, Kuo CC. 1998. Human mannose-binding protein 721 21.
- inhibits infection of HeLa cells by Chlamydia trachomatis. Infect Immun 66:1607–12. 722
- Hjelholt A, Christiansen G, Sørensen US, Birkelund S. 2013. IgG subclass profiles in 22. 723
- normal human sera of antibodies specific to five kinds of microbial antigens. Pathog Dis 724
- **67**:206–213. 725
- 23. Su H, Spangrude GJ, Caldwell HD. 1991. Expression of FcyRIII on HeLa 229 cells: 726
- Possible effect on in vitro neutralization of Chlamydia trachomatis. Infect Immun. 727
- American Society for Microbiology (ASM). 728
- Scidmore MA, Rockey DD, Fischer ER, Heinzen RA, Hackstadt T. 1996. Vesicular 729 24.
- 730 interactions of the Chlamydia trachomatis inclusion are determined by chlamydial early
- protein synthesis rather than route of entry. Infect Immun **64**:5366–5372. 731
- 25. Gigli I, Fujita T, Nussenzweig V. 1979. Modulation of the classical pathway C3 732
- convertase by plasma proteins C4 binding protein and C3b inactivator. Proc Natl Acad 733
- Sci 76:6596-6600. 734
- Berggard K, Johnsson E, Morfeldt E, Persson J, Stalhammar-Carlemalm M, 735 26.
- **Lindahl G.** 2001. Binding of human C4BP to the hypervariable region of M protein: a 736
- molecular mechanism of phagocytosis resistance in Streptococcus pyogenes. Mol 737
- Microbiol 42:539-551. 738

- 739 27. Prasadarao N V., Blom AM, Villoutreix BO, Linsangan LC. 2002. A Novel
- Interaction of Outer Membrane Protein A with C4b Binding Protein Mediates Serum 740
- Resistance of *Escherichia coli* K1. J Immunol **169**:6352–6360. 741
- Watford WT, Ghio AJ, Wright JR. 2000. Complement-mediated host defense in the 742 28.
- lung. Am J Physiol Lung Cell Mol Physiol 279:L790-8. 743
- 29. Geier H, Celli J. 2011. Phagocytic Receptors Dictate Phagosomal Escape and 744
- Intracellular Proliferation of Francisella tularensis. Infect Immun 79:2204–2214. 745
- 30. Bode J, Dutow P, Sommer K, Janik K, Glage S, Tummler B, Munder A, Laudeley 746
- R, Sachse KW, Klos A. 2012. A new role of the complement system: C3 provides 747
- protection in a mouse model of lung infection with intracellular Chlamydia psittaci. 748
- PLoS One 7:e50327. 749
- 750 31. Dutow P, Fehlhaber B, Bode J, Laudeley R, Rheinheimer C, Glage S, Wetsel RA,
- Pabst O, Klos A. 2014. The Complement C3a Receptor Is Critical in Defense against 751
- Chlamydia psittaci in Mouse Lung Infection and Required for Antibody and Optimal T 752
- Cell Response. J Infect Dis **209**:1269–1278. 753
- 32. Martin U, Bock D, Arseniev L, Tornetta MA, Ames RS, Bautsch W, Köhl J, Ganser 754
- 755 **A, Klos A.** 1997. The human C3a receptor is expressed on neutrophils and monocytes,
- but not on B or T lymphocytes. J Exp Med **186**:199–207. 756
- Chenoweth DE, Hugli TE. 1978. Demonstration of specific C5a receptor on intact 757 33.

- 758 human polymorphonuclear leukocytes. Proc Natl Acad Sci U S A 75:3943–3947. Brekke O-L, Christiansen D, Fure H, Fung M, Mollnes TE. 2007. The role of 759 34.
- complement C3 opsonization, C5a receptor, and CD14 in E. coli-induced up-regulation 760 761 of granulocyte and monocyte CD11b/CD18 (CR3), phagocytosis, and oxidative burst in
- human whole blood. J Leukoc Biol 81:1404–1413. 762
- Mollnes TE, Brekke O-L, Fung M, Fure H, Christiansen D, Bergseth G, Videm V, 763 35.
- Lappegard KT, Kohl J, Lambris JD. 2002. Essential role of the C5a receptor in E coli-764
- induced oxidative burst and phagocytosis revealed by a novel lepirudin-based human 765
- 766 whole blood model of inflammation. Blood **100**:1869–1877.
- Sengeløv H, Kjeldsen L, Kroeze W, Berger M, Borregaard N. 1994. Secretory 36. 767
- 768 vesicles are the intracellular reservoir of complement receptor 1 in human neutrophils. J
- Immunol **153**:804–10. 769
- 37. Crowell RE, Van Epps DE. 1990. Nonsteroidal antiinflammatory agents inhibit 770
- upregulation of CD11b, CD11c, and CD35 in neutrophils stimulated by formyl-771
- methionine-Leucine-phenylalanine. Inflammation 14:163–171. 772
- 38. Furtado PB, Huang CY, Ihyembe D, Hammond RA, Marsh HC, Perkins SJ. 2008. 773
- 774 The Partly Folded Back Solution Structure Arrangement of the 30 SCR Domains in
- Human Complement Receptor Type 1 (CR1) Permits Access to its C3b and C4b Ligands. 775
- 776 J Mol Biol **375**:102–118.

- 777 39. Rajeeve K, Das S, Prusty BK, Rudel T. 2018. Chlamydia trachomatis paralyses neutrophils to evade the host innate immune response. Nat Microbiol 3:824–835. 778
- 40. Wolf K, Fischer E, Hackstadt T. 2005. Degradation of Chlamydia pneumoniae by 779 780 peripheral blood monocytic cells. Infect Immun 73:4560–70.
- Martinez-Pomares L. 2012. The mannose receptor. J Leukoc Biol 92:1177–1186. 781 41.
- 42. Lausen M, Christiansen G, Bouet Guldbæk Poulsen T, Birkelund S. 2019. 782
- Immunobiology of monocytes and macrophages during Chlamydia trachomatis infection. 783
- Microbes Infect 21:73-84. 784
- Airenne S, Surcel HM, Alakärppä H, Laitinen K, Paavonen J, Saikku P, Laurila A. 785 43.
- 1999. Chlamydia pneumoniae infection in human monocytes. Infect Immun 67:1445– 786
- 787 1449.
- Prain CJ, Pearce JH. 1989. Ultrastructural studies on the intracellular fate of 44. 788
- Chlamydia psittaci (strain guinea pig inclusion conjunctivitis) and Chlamydia 789
- trachomatis (strain lymphogranuloma venereum 434): modulation of intracellular events 790
- and relationship with endocytic mechan. J Gen Microbiol 135:2107–23. 791
- Birkelund S, Lundemose AG, Christiansen G. 1988. Chemical cross-linking of 792 45.
- Chlamydia trachomatis. Infect Immun **56**:654–659. 793
- 794 46. Knudsen K, Madsen AS, Mygind P, Christiansen G, Birkelund S. 1999.
- Identification of two novel genes encoding 97- to 99-kilodalton outer membrane proteins 795

815

790		of Chiamydia pheumomae. Threet minun <b>67</b> .575–83.
797	47.	Lausen M, Christiansen G, Karred N, Winther R, Poulsen TBG, Palarasah Y,
798		<b>Birkelund S</b> . 2018. Complement C3 opsonization of Chlamydia trachomatis facilitates
799		uptake in human monocytes. Microbes Infect 20:328–336.
800		
801		
802		
803		
804		
805		
806		
807		
808		
809		
810		
811		
812		
813		

822

823

824

825

826

827

830

831

832

833

834

835

836

837

838

## 817 Figure 1 818 Complement opsonization of C. pneumoniae in non-immune serum. Purified C. pneumoniae EBs were incubated 819 820 821

FIGURE LEGENDS

in A) non-immune serum (NHS-) or B) heat-inactivated non-immune serum (HIHS-) and analyzed by immunoelectron microscopy (IEM) using anti-C3c and anti-rabbit 10 nm colloidal gold as primary and secondary antibodies, respectively. C) Gold deposition on each bacterium was quantified relative to the background gold level for each condition (NHS- and HIHS-). D) Purified C. pneumoniae EBs were subjected to western blot analysis and labeled against C3c. C. pneumoniae EBs were incubated in E) NHS- or F) HIHS- and subjected to IEM using anti-C4c as primary antibody. G) Complement C4 deposition was quantified as described for panel C). H) Western blot analysis of complement C4 deposition on C. pneumoniae incubated in NHS- or HIHS-. Western blot analysis was repeated three times and representative blots are shown. IEM images were captured from at least 8 random fields for each sample in one experiment. For each bacterium, a bacterium-to-

828 background gold deposition ratio was calculated and plotted with each dot representing one chlamydial 829 organism. The median ratio is presented as black lines. Scale bars indicate 200 nm.

## Figure 2

Antibody- and complement opsonization of C. pneumoniae in immune serum. C. pneumoniae (5x10<sup>5</sup> IFU/well) were grown in in HeLa cells for 48 hours and chlamydial inclusions were immunofluorescently stained using two-fold serial dilutions of A) immune serum or B) non-immune serum as primary antibody. Purified C. pneumoniae EBs incubated in C) heat-inactivated immune serum (HIHS+) or D) heat-inactivated non-immune serum (HIHS-) were immuno-labeled with anti-human IgG 10 nm colloidal gold and subjected to immunoelectron microscopy (IEM). E) From IEM images, chlamydial gold deposition, for each bacterium, was quantified relative to the background gold level. Purified C. pneumoniae EBs were incubated in F) immune

840

841

842

843

844

845

846

847

848

849

850

851

852

853

854

855

856

857

858

859

860

861

serum (NHS+) or G) heat-inactivated immune serum (HIHS+) and analyzed by IEM using anti-C3c and antirabbit 10 nm colloidal gold as primary and secondary antibodies, respectively. H) Gold deposition in IEM images was quantified as described for panel E. I) Purified C. pneumoniae EBs were subjected to western blot analysis and labeled against C3c. J-M) C. pneumoniae were treated as described in panel F-I except bacteria were labeled using an anti-C4c antibody. For immunofluorescence microcopy, each serum was tested in four different dilutions and images were captured from five random fields for each dilution. The experiment was repeated twice. In IEM, a bacterium-to-background gold deposition ratio was calculated for each bacterium and plotted, with each dot representing one chlamydial organism. The median ratio is presented as black lines. IEM images were captured from at least 8 random fields for each sample in one experiment. Western blot analysis was repeated three times and representative blots are shown. Scale bars indicate 10 µm (A,B) and 200 nm (C,D,F,G,J,K).

Figure 3

Formation of membrane attack complex (MAC) on C. pneumoniae. Purified C. pneumoniae EBs were incubated in immune- and non-immune serum and processed for IEM. Images show A) C. pneumoniae incubated in immune-serum (NHS+) and negatively stained with PTA. B) C. pneumoniae incubated in immune-serum (NHS+) and negatively stained with PTA and C) C. pneumoniae incubated in non-immune serum (NHS-) and immuno-gold labeled against C5b-9. Area with disintegrated bacterial morphology was enlarged (hatched boxes) demonstrating 10 nm pore-like structures (yellow arrowheads) (B+C) in close proximity to gold particles (C). D) C. pneumoniae incubated in heat-inactivated immune-serum (HIHS+) and immuno-gold labeled against C5b-9. Anti-mouse 10 nm colloidal gold was used as secondary antibody. IEM images were used to quantify gold deposition on C. pneumoniae incubated in E) non-immune serum and F) immune serum. For each chlamydial organism, the gold particle deposition was quantified by calculating a

Downloaded from http://iai.asm.org/ on April 15, 2020 at Aalborg University Library

bacteria-to-background ratio and the ratios were used to create scatter plots. Each dot represents the ratio from one chlamydial organism and the black lines show the median ratio. Scalebars indicate 200 nm. HIHS-: heatinactivated non-immune serum.

865

866

867

868

869

870

871

872

873

874

875

876

862

863

864

## Figure 4

Serum neutralization of C. pneumoniae EBs. C. pneumoniae inoculum were incubated in immune-serum (NHS+), non-immune serum (NHS-), heat-inactivated immune-serum (HIHS+), heat-inactivated non-immune serum (HIHS-) or HIHS- supplemented with 1.5 mg/ml IgG from immune-serum (HIHS-+IgG) for 30 min and used to infect HeLa cells. HeLa cells were inoculated with 10.8x10<sup>4</sup> inclusion forming units (IFU) of NHSopsonized C. pneumoniae and 1.2x10<sup>4</sup> IFU of HIHS-opsonized C. pneumoniae. IFU were quantified by immunofluorescence staining of chlamydial inclusions. Images were captured from seven random fields in each sample using a 16X objective. Data were obtained from duplicate samples from three independent experiments. All data are presented as mean ± SD. Differences between means were analyzed by Welch's ANOVA with Games-Howell multiple comparisons test. P-values < 0.05 were considered statistically significant and denoted with an asterix (\*).

Downloaded from http://iai.asm.org/ on April 15, 2020 at Aalborg University Library

877

878

879

880

881

882

883

## Figure 5

Opsonophagocytosis of C. pneumoniae in monocytes and neutrophils. The percentage of C. pneumoniae-positive A) monocytes and B) neutrophils incubated with C. pneumoniae at MOI=10 in non-immune serum was quantified by flow cytometry. The combined role of complement and anti-C. pneumoniae IgG in C) monocyte and D) neutrophil phagocytosis was tested using immune serum. Heat-inactivated non-immune serum and heatinactivated non-immune serum supplemented with the IgG fraction from immune serum was used as control to

885

886

887

888

889

890

891

892

893

894

895

896

897

898

899

900

901

902

903

904

905

906

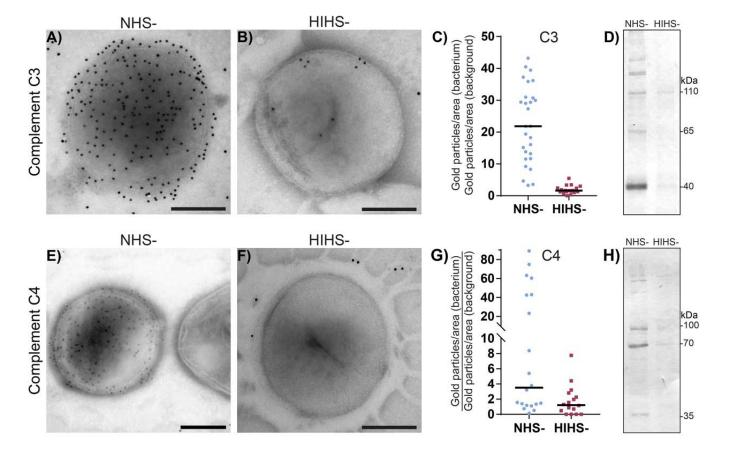
907

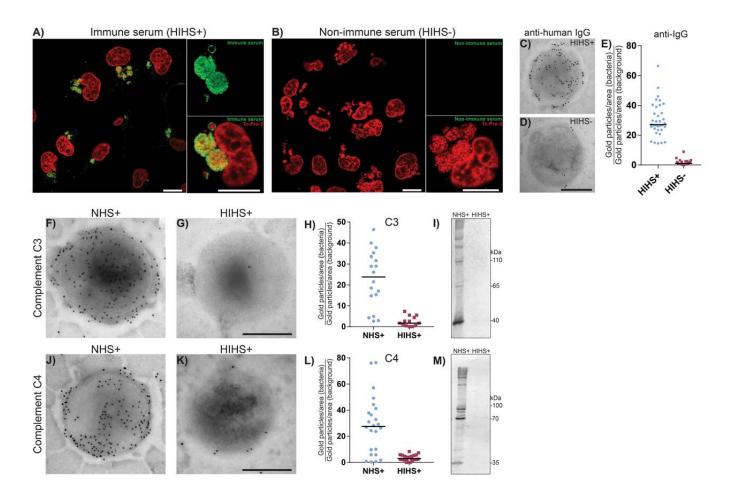
determine the role of IgG in phagocytosis in E) monocytes and F) neutrophils. The percentage of C. pneumoniae-positive G) monocytes and H) neutrophils incubated with C. pneumoniae at MOI=1 in immune serum and non-immune serum. Data were obtained from duplicate samples from three independent experiments except for E) + F) which was obtained from duplicate samples from two independent experiments. A minimum of 8,000 gated events were obtained from each sample. All data are presented as mean ± SD. One-way ANOVA with Tukey's post hoc test, Welch's ANOVA with Games-Howell multiple comparison test or Welch's t-test were used to compare column means. P-values < 0.05 were considered statistically significant and denoted with an asterix (\*). NHS+: Immune serum, NHS-: Non-immune serum, HIHS+: heat-inactivated immune serum, HIHS-: heat-inactivated non-immune serum, HIHS-+ IgG: heat-inactivated non-immune serum supplemented with IgG fraction from immune serum.

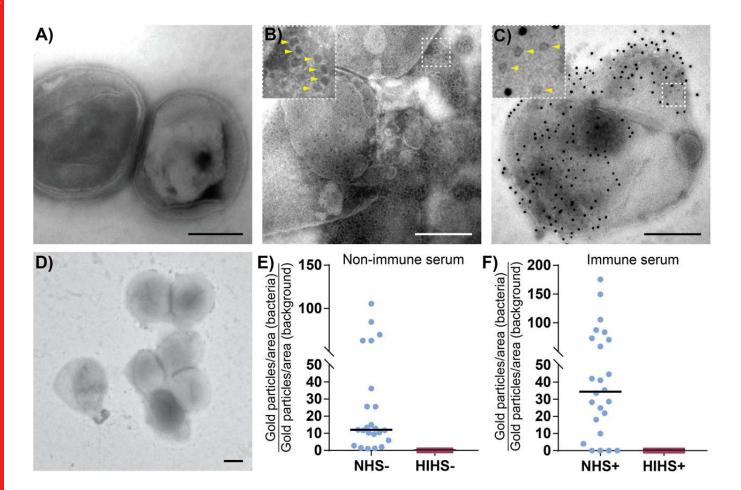
Figure 6

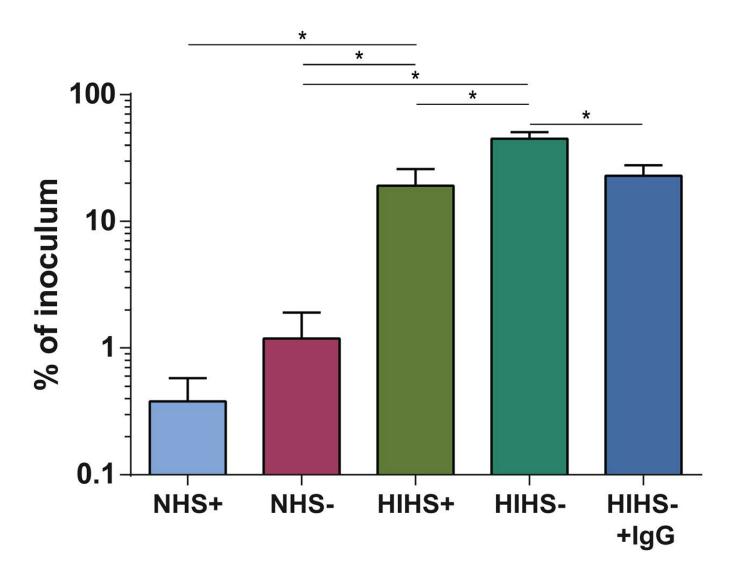
Intracellular neutralization of opsonized C. pneumoniae in PBMCs and neutrophils. C. pneumoniae (MOI=10) were incubated with A) PBMCs and B) neutrophils under different culture conditions for 30 min and cell lysates were prepared by ultrasonication. Lysates were used to infect HeLa cell monolayers and inclusion forming units (IFU) was enumerated after 48 hours by immunofluorescence microscopy. Intracellular localization of C. pneumoniae in monocytes after 30 min was investigated by immunofluorescence staining and confocal microscopy of C) C. pneumoniae and D) LAMP1. Frame E) shows an overlay image. F) Monocyte incubated with mock control. Confocal microscopy was repeated twice for all four (NHS+/NHS-/HIHS+/HIHS-) conditions and images were captured from five random fields in each sample. Quantitative data were obtained from duplicate samples from three independent experiments. Data are presented as mean ± SD. Differences between means were analyzed by Welch's ANOVA with Games-Howell multiple comparisons test. P-values < 0.05 were considered statistically significant and denoted with an asterix (\*). Scale

bar indicates 5 $\mu m$ . NHS+: Immune serum, NHS-: Non-immune serum, HIHS+: heat-inactivated
immune serum, HIHS-: heat-inactivated non-immune serum









Downloaded from http://iai.asm.org/ on April 15, 2020 at Aalborg University Library

